Improvement of light to biomass conversion by de-regulation of light-harvesting protein translation in *Chlamydomonas reinhardtii*

J. Beckmann[a], F. Lehr[b], G. Finazzi[c], B. Hankamer[d], C. Posten[b], L. Wobbe[e], O. Kruse[a,*]

[a] *Department of Biology, Algae Biotech Group, University Bielefeld, 33501 Bielefeld, Germany*
[b] *Institute of Engineering in Life Sciences, University of Karlsruhe (TH), 76128 Karlsruhe, Germany*
[c] *UPR 1261-CNRS, Institut de Biologie Physico-Chimique, 75005 Paris, France*
[d] *Institute for Molecular Bioscience, University of Queensland, St. Lucia Campus, Brisbane, QLD 4072, Australia*
[e] *Wolfson Laboratories, Dept. of Biological Sciences, Imperial College London, London SW7 2AZ, UK*

ABSTRACT

The efficient use of microalgae to convert sun light energy into biomass is limited by losses during high light illumination of dense cell cultures in closed bioreactors. Uneven light distribution can be overcome by using cell cultures with smaller antenna sizes packed to high cell density cultures, thus allowing good light penetration into the inner sections of the reactor. We engineered a new small PSII antenna size *Chlamydomonas reinhardtii* strain with improved photon conversion efficiency and increased growth rates under high light conditions. We achieved this goal by transformation of a permanently active variant NAB1* of the LHC translation repressor NAB1 to reduce antenna size via translation repression. NAB1* expression was demonstrated in *Stm6Glc4T7 (T7)*, leading to a reduction of LHC antenna size by 10–17%. *T7* showed a ~50% increase of photosynthetic efficiency (ΦPSII) at saturating light intensity compared to the parental strain. *T7* converted light to biomass with much higher efficiencies with a ~50% improved mid log growth phase. Moreover, *T7* cultures reached higher densities when grown in large-scale bioreactors. Thus, the phenotype of strain *T7* may have important implications for biotechnological applications in which photosynthetic microalgae are used for large-scale culturing as an alternative plant biomass source.

© 2009 Elsevier B.V. All rights reserved.

1. Introduction

In order to achieve optimal growth conditions, photosynthetic organisms are able to acclimate to sunlight quality and quantity by modulating their photosynthetic apparatus, and in particular the size and composition of their light-harvesting antenna systems (LHC) (Escoubas et al., 1995; Durnford and Falkowski, 1997; Yang et al., 2001). In the case of the unicellular microalga *Chlamydomonas reinhardtii* the LHC complex consists of at least 20 members of a large extended family of chlorophyll-binding protein subunits. Nine of these proteins are predicted to be predominantly associated with photosystem (PS) II and therefore are being referred to as LHCII proteins (Elrad and Grossman, 2004) and have been identified at the protein level by mass spectrometry (Stauber et al., 2003; Turkina et al., 2006). Although the LHCII proteins are structurally very similar, it is likely that individual gene products have specific functions. However, up to now only two isoforms have been clearly

linked to a specific function in *C. reinhardtii*. The knock-out of the isoform LHCBM1 was shown to somehow impair the development of non-photochemical quenching (NPQ) of excitation energy in *C. reinhardtii* (Elrad et al., 2002). LHCBM9 was shown to be highly up-regulated under certain stress conditions such as sulphur depletion and anaerobiosis (Nguyen et al., 2008).

In general, the regulation of LHCII expression is of importance to allow the photosynthetic machinery to cope with fluctuating ambient light conditions in order to avoid photo-oxidative damage (Anderson and Andersson, 1988). This is known to occur at many levels including transcription initiation (Maxwell et al., 1995; Millar et al., 1995), and post-transcriptional regulation (Flachmann and Kühlbrandt, 1995; Lindahl et al., 1995; Durnford et al., 2003). In addition, we recently showed that LHC translation control in *C. reinhardtii* via the cytosolic RNA-binding protein NAB1 plays an important role in regulating the size and composition of the LHCII antenna (Mussgnug et al., 2005). NAB1 binds distinct mRNAs of *LHCBM* genes *in vitro* and *in vivo*. RNA-binding by NAB1 prevents LHCBM translation via sequestration of the message in translationally silent messenger ribonucleoprotein complexes (mRNPs) and RNA co-immunoprecipitation experiments revealed that NAB1 binds the isoform 6 with a very high affinity. The absence of functional NAB1 in a knock-out mutant generated by random

* Corresponding author. University of Bielefeld, Fakulty of Biology, Algae BioTech Group, Universitätsstr. 25, 33615 Bielefeld, Germany. Tel.: +49 521 1065611; fax: +49 521 10689036.
E-mail address: olaf.kruse@uni-bielefeld.de (O. Kruse).

insertional mutagenesis of the nuclear genome is accompanied by a 30–40% increase of the antenna size at PSII (Mussgnug et al., 2005). Very recently we were able to show that NAB1 activity is redox-controlled and regulated via two cysteine residues, Cys181 and Cys226 within its C-terminal *RNA Recognition Motif* (RRM). The replacement of these cysteines by serine results in a permanently active form of NAB1 which finally leads to a phenotype with a 20% reduced antenna system at PSII (Wobbe et al., unpublished).

Besides their essential role in light capture antenna proteins are important to avoid photo-oxidative damage. Certain LHC subunits are needed to dissipate light energy as heat or fluorescence via non-photochemical quenching when solar irradiation exceeds photosynthetic capacity (Müller et al., 2001). Although this protection mechanism is an essential survival strategy under natural conditions, it can reduce the photon conversion efficiency (PCE) and biomass production rates (Prince and Kheshgi, 2005), particularly in dense cultures of microalgae. High PCE rates however need to be achieved in biotechnology applications using closed algae bioreactor systems for optimal biomass production yields, in particular under high light (Polle et al., 2002, 2003; Kruse et al., 2005). Consequently, we and others aimed to show that a reduction of the light-harvesting antenna size, improves the efficiency of the culture, by minimizing heat and fluorescence losses at the culture surface and improving light penetration into the bioreactor. This in turn results in faster growth under high light conditions and indeed was shown to reduce photoinhibition in certain cases (Mussgnug et al., 2007; Melis, 1999; Prince and Kheshgi, 2005; Neidhardt et al., 1998).

In this work, we intended to engineer a new small PSII antenna size *C. reinhardtii* strain with improved photon conversion efficiency and increased growth rates under high light conditions. To achieve this goal we aimed to construct a mutant in which we can fine-tune and acclimate the antenna size according to its physiological growth state and in dependence to fluctuating illumination conditions. Our strategy included the transformation of permanently active variations of the LHC II translation repressor NAB1 to reduce LHC antenna size via translation repression.

2. Materials and methods

2.1. Strains and culture conditions

Liquid cultures of *C. reinhardtii* mutant strain *Stm6Glc4* (Doebbe et al., 2007) and *Stm6Glc4* derivatives were grown in continuous white light in TAP media (Tris Acetate Phosphate, $40 \mu mol\, m^{-2}\, s^{-1}$ white light) and in HSM (High Salt Medium) (Sueoka et al., 1967) purged with 2% CO_2 under continuous illumination ($700 \mu mol\, m^{-2}\, s^{-1}$ white light). Media for mixotrophic (TAP) and photoautotrophic growth (HSM) were prepared as described (Harris, 1989; Sueoka et al., 1967). TAP agar with 100 μM emetine (Sigma) was prepared to screen positive transformants.

Autotrophic cell growth was tested in minimal medium (HSM) purged with 2% CO_2 in continuous white light under elevated conditions ($700 \mu mol\, m^{-2}\, s^{-1}$). 200 mL volume of HSM were inoculated with *Stm6Glc4* and *Stm6Glc4T7* ($OD_{750\,nm} = 0.05 = 1 - 1.5 \times 10^6$ cells mL^{-1}). Growth rates were determined by monitoring the photometric absorption ($OD_{750\,nm}$) and by counting the cells. The cells were counted using the *Bürker* cell counting chamber (VWR, Germany).

The photo-bioreactor used was a standard 2.4 L stirred tank reactor. To achieve good light penetration of the algae suspension, a high height/diameter-ratio of 3.2 was used for the glass vessel. The photo-bioreactor was equipped with a customized LED-lighting system which consisted of two printed circuit board half shells which were assembled with warm white SMD-LEDs. Due to the rounded geometry of the half shells and the special radiation angle of the LEDs, the emitted light is focused to the centre of the reactor (lens effect) and therefore compensates the light intensity drop towards the centre of the reactor caused by the mutual shading effect of the algae cells. Together with the small reactor diameter this results in an almost homogenous light distribution inside the reactor, even at higher biomass concentrations. To be able to achieve high light intensities up to 2000 $\mu mol\, m^{-2}\, s^{-1}$, the LED half shells were equipped with a double jacket for water cooling at the back side. Autotrophic cell growth experiments were carried out in 1.8 L TAP-medium without acetate. The cell suspension was purged with sterile 3% CO_2 in air at a flow rate of 35 mL L^{-1} min which was controlled via two mass flow controllers (MKS Mass-FLO). The bio-suspension was agitated at 250 rpm by two six-bladed Rushton turbines with a stirrer to vessel diameter-ratio of 0.6. Temperature was kept constant at 25 °C. All parameters were recorded and controlled online via a routine written in LabView (National Instruments). The oxygen and carbon dioxide content of the exhaust gas was measured via a Maihak Multor 610 system. The reactor was inoculated with a pre-culture grown in TAP on an orbital shaker at 25 °C with continuous white light at 100 $\mu mol\, m^{-2}\, s^{-1}$. The starting biomass was adjusted to approximately 0.05 g L^{-1}. Dry weight of biomass was determined by centrifuging 25 mL bio-suspension for 10 min at $14,000 \times g$ (Hettich Universal 30RF) in stainless steel centrifugation tubes which has been dried and weighed out before. The supernatant was discarded and the pellet washed two times with deionized water and centrifuged again. Afterward the pellet was dried for 24 h at 80 °C, cooled down in dessicator and weighed out again. Every sample was determined three times.

2.2. Mutant constructions and genetic analysis

Mutants were generated by glass bead co-transformation with plasmid *pGDNG3/Cys(181/226)Ser* and *p613* (Kindle, 1990; Nelson et al., 1994) and selected on TAP agar plates containing emetine, to test for resistance to the drug.

Plasmid *pGDNG3* was constructed by inserting the wild-type (WT) *NAB1* gene into the NdeI and EcoRI cloning sites of plasmid *pGenD* (Fischer and Rochaix, 2001). The plasmid *pGDNG3/Cys(181/226)Ser* was generated by site-specific replacement of thymine by adenine at positions 541 and 676 (*QuikChange®Site-Directed Mutagenesis Kit*; Stratagene). Double mutants were generated by two successive mutagenesis reactions and all generated constructs were sequenced within the entire *NAB1* coding sequence. Exchange of both redox-sensitive cysteines of NAB1 to serine by means of site-specific mutagenesis generates a translation repressor which is arrested in a permanently active state (Wobbe et al., unpublished).

2.3. Isolation of nucleic acids

Escherichia coli DH5α cells were used as hosts for all plasmids. Isolation was performed with *PeqLab* Plasmid Miniprep Kit I. For PCR with genomic DNA, *C. reinhardtii* genomic DNA was purified using the phenol/chloroform extraction described in (Sambrook and Russel, 2001).

2.4. PCR with genomic DNA

All oligonucleotides for PCR reactions were designed with *Primer 3* (http://cbr-rbc.nrc-cnrc.gc.ca/cgi-bin/primer3_www.cgi) and synthesized by *Sigma Genosys*. PCR analysis of *pGDNG3/Cys(181/226)Ser* integration was performed with oligonucleotides *PsaD5′UTR_Nab1fow2* (5′gcggcgtgattattggtatt3′), *PsaD5′UTR_Nab1rev2* (5′gatccactgcagcaccact3′), *Nox3F2* (5′cagctcaaggaccacttcaa3′) and *Nox3R2* (5′acggcaaactctcacatgg 3′) and 300 ng of isolated genomic DNA.

2.5. RNA Isolation and (semi-) quantitative real time-PCR

Total RNA from *C. reinhardtii* cultures was isolated according to (Chomczynski and Sacchi, 1987). For the reverse transcription (RT) PCR the complementary DNA was synthesized from 5 μg DNaseI treated total RNA of *Stm6Glc4* and *Stm6Glc4 T7* using 2 μg template specific oligonucleotide *qRT_3'NAB*1_rev* (5′cccgtatcaatcagcgaa3′) and *Actin qPCR rp 102* (5′ggagttgaaggtggtgtcgt3′) and M-MLV-Reverse Transcriptase (Promega) according to (Promega Usage Information). After reverse transcription standard PCR was initiated with oligonucleotides of *qRT_3'NAB*1_fow* (5′cgacaagttgaacaacagcc3′), *qRT_3'NAB*1_rev* (5′cccgtatcaatcagcgaa3′), *Actin qPCR lp102* (5′cgctggagaagacctacgag3′), *Actin qPCR rp 102* (5′ggagttgaaggtggtgtcgt3′).

Quantitative real time-PCR (RT-Q-PCR) was performed with the SensiMix™ One-Step Kit (*Quantace*). Each reaction contained 12.5 μL SensiMix One-Step, 0.5 μL SYBR® Green I Solution, 0.5 μL 10 U/μL RNase Inhibitor, 300 ng of RNA, 200 nM of each gene-specific primer, H_2O was added to a final volume of 25 μL. PCR cycling conditions included a first cDNA synthesis step at 49 °C for 30 min, an initial polymerase activation step at 95 °C for 10 min followed by 44 PCR cycles at 95 °C for 15 s, 60 °C for 30 s and 72 °C for 40 s, and a final melting step of 60–90 °C each for 30 s. PCR was performed with oligonucleotides of *qRT_3'NAB*1_fow* (5′cgacaagttgaacaacagcc3′), *qRT_3'NAB*1_rev* (5′cccgtatcaatcagcgaa3′), *Actin qPCR lp102* (5′cgctggagaagacctacgag3′), *Actin qPCR rp 102* (5′ggagttgaaggtggtgtcgt3′), *NAB1-CDS lp* (5′gctcaaggaccacttcaagg3′), *NAB1-CDS rp* (5′gtcgatttggctgttgttca3′).

Analysis was carried out using a Real Time-Cycler (DNA Engine Opticon™ Detector, MJ Research) with the Dissociation and Opticon Monitor™ software. Real time DNA amplification was monitored and analyzed using the Sequence Detector 1.9.1 software (PerkinElmer Life Sciences). Gene expression levels were calculated in relation to *β-Actin* according to (Protocols & Application Guide, Promega).

2.6. Western blot analysis

Proteins were extracted with denaturing sample buffer (Schägger and Jagow, 1987) and separated by SDS-PAGE in 10% Tris-Tricine gels (Schägger and Jagow, 1987). Western blotting was performed according to (Towbin et al., 1979). LHC-specific antibodies raised against higher plants LHCB proteins were used in conjunction with ECL™-anti-Rabbit IgG (HRP-linked whole Ab from donkey). For the protein samples, 200 mL *Stm6Glc4* and *Stm6Glc4 T7* cells were grown autotrophically to mid log phase, adjusted to equal cell densities (1.55×10^7 cells) and centrifuged ($2000 \times g$, 2 min). The pellet was re-suspended in 117.5 μL H_2O containing 1 μL Benzonase (Sigma). The final sample volume loaded on the gel was 20 μL and 27.5 μL for *Stm6Glc4* for *Stm6Glc4T7*, respectively.

2.7. Chlorophyll fluorescence and oxygen evolution measurements

The chlorophyll parameters were determined at room temperature (Mini-PAM, Walz). F_v/F_m was determined after dark incubation of cell suspension (15 μg ChlmL^{-1}) for 5 min by recording of F_o and F_m (the latter after application of a saturating light pulse of 15 000 μmol m^{-2} s^{-1}) and calculation of $F_v/F_m = (F_m - F_o)/F_m$ (Maxwell and Johnson, 2000). Photosynthetic quantum yield (ΦPSII) was determined by illuminating cell suspension (15 μg Chl mL^{-1}) with actinic white light under increasing intensities. Fluorescence parameters were recorded and quantum yield calculated [ΦPSII = $(F'_m - F_t)/F'_m$ (Maxwell and Johnson, 2000)].

Alternatively, fluorescence was measured using a home built fluorimeter. Excitation was provided by LEDs with a peak emission at 520 nm (10 nm FWHM, full width at half maximum), and fluorescence was detected in the near IR region. The estimate of the PSII antenna size was obtained by measuring fluorescence-induction kinetics in the presence of saturating concentrations of DCMU, to block reoxidation of the PSII electron acceptor Q_A. We measured the time *t* at which the variable fluorescence yield was ~2/3 of the maximum value. As an average of 1 photon per PSII centre is absorbed at time *t* (see e.g. Joliot and Joliot, 2005), its value provides an estimate of the number of absorbed photons, with a precision of ±10%.

Oxygen evolution measurements were performed using a Clark-type oxygen electrode (HansaTech). Cell cultures were grown for 3 days with 40 μmol m^{-2} s^{-1} and adjusted to identical cell densities (7×10^6 cells mL^{-1}). Apparent O_2 production was measured with a Clark-type oxygen electrode after addition of NaHCO$_3$ (10 mM final concentration) with increasing light intensities (16, 50, 90, 270, 923 μmol m^{-2} s^{-1}) at 25 °C for 3 min. Light saturation curves of photosynthesis were plotted on a per cell basis. Respiration was determined at the end of each light period by dark incubation for 3 min. Gross photosynthetic rates were calculated by subtracting respiration from net O_2 production rates.

3. Results

In this work we aimed to improve sunlight to biomass conversion in microalgae by constructing new *C. reinhardtii* strains with smaller light-harvesting antenna systems. Based on our knowledge on cytosolic translation control of light-harvesting antenna proteins in this organism, we intended to achieve this goal by transformation of a permanently active variant of the LHC translation repressor NAB1 (Mussgnug et al., 2005). The high H_2 production strain *Stm6Glc4* (Doebbe et al., 2007) was selected as the target strain to optimize its light to biomass conversion efficiency. The isolated strain *Stm6Glc4* derives from the high H_2 production mutant *Stm6*, a strain that has been previously isolated and characterised as a strain with a modified respiratory metabolism, large starch reserves and perturbed cyclic electron transfer around PSI (Kruse et al., 2005). As a further improvement, the modified strain *Stm6Glc4* can use externally supplied glucose for heterotrophic growth in the dark and in the light. More importantly, external glucose supply increases the H_2 production capacity in this strain *Stm6Glc4* to ~150% of that of the high H_2 producing strain *Stm6*.

3.1. Construction of Stm6Glc4 transformants carrying a permanently active variant of the LHC translation repressor NAB1

Recently we found that oxidation or alkylation of the two cysteines within the NAB1 protein is accompanied by a decrease in RNA-binding affinity for the target mRNA sequence of LHC II subunits. In line with these findings, the exchange of the cysteines to serine resulted in a permanently active variant of the translation repressor NAB1 and finally in a reduction of the LHCII antenna size (Wobbe et al., unpublished). Therefore, we constructed the vector plasmid *pGDNG3/Cys(181/226)Ser* which was designed to express a mutagenized NAB1 (NAB1*) coding sequence, in which the C-terminal cysteines at positions 181 and 226 have been replaced by serines via a site-directed mutagenesis approach (Wobbe et al., unpublished). In this vector, NAB1* expression is under the control of the flanking regions of the *C. reinhardtii PsaD* gene (Fischer and Rochaix, 2001). *pGDNG3/Cys(181/226)Ser* was then co-transformed with a second vector, *p613* into the high H_2 production strain *Stm6Glc4* (Doebbe et al., 2007). The transformation into this specific strain should enable us in the future to combine improved light to biomass conversion with high H_2 production. The plasmid *p613* contains the dominant selectable marker gene *CRY1* and therefore allows selection of positive transformants with the antibiotic emetine (Nelson et al., 1994). 104 emetine-resistant transformants were
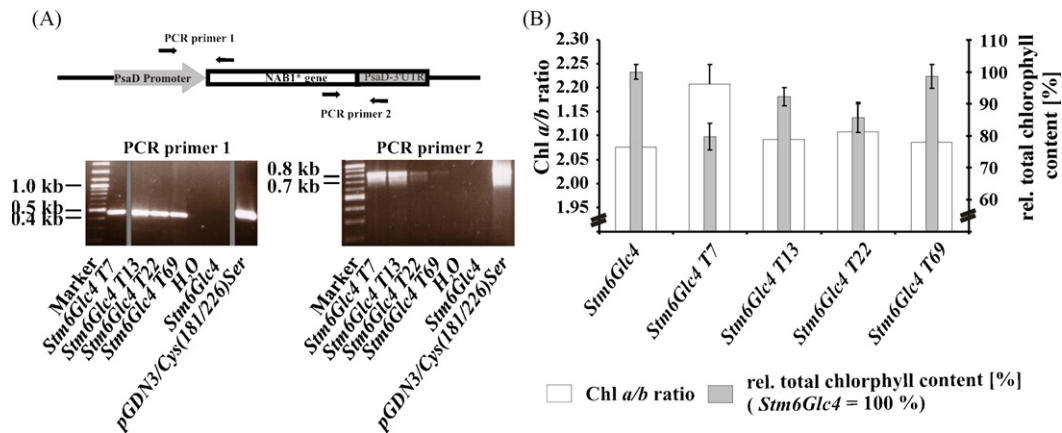
Fig. 1. Screening and identification of NAB1* insertion mutants in the genome of *C. reinhardtii* strain *Stm6Glc4*. (A) PCR confirmation of emetine-resistant *Stm6Glc4* transformants for co-integration of the NAB1* containing plasmid *pGDN3/Cys(181/226)Ser* using two different NAB1* specific PCR primer pairs and genomic DNA of individual transformants (*T7*, *T13*, *T22* and *T69*). PCR primer pair 1 binds to a region within the *PsaD* promoter of the plasmid *pGDN3/Cys(181/226)Ser* and in the first intron of the NAB* gene, primer pair 2 recognises a sequence within the second last exon of the NAB* gene and the 3′ region of the plasmid *pGDN3/Cys(181/226)Ser* thus enabling confirmation of nuclear insertion of the complete NAB* gene and to distinguish endogenous NAB1 and NAB1*. PCR primer 1: *PsaD5′UTR_Nab1fow2* (5′gcggccgtgattattggtatt3′), *PsaD5′UTR_Nab1rev2* (5′gatccactgcagcaccact3′), product size: 471 bp PCR primer 2: *Nox3F2* (5′cagctcaaggaccacttcaa3′) and *Nox3R2* (5′acggcaaactctcacatgg3′) product size: 808 bp. (B) Total chlorophyll content of different NAB1* mutants relative to the parental strain *Stm6Glc4* (right *y*-axis; grey bars; *Stm6Glc4*=100%) and Chl *a*/*b* ratios of the different mutants and *Stm6Glc4* strain (left *y*-axis; white bars). The data represent values of three independent chlorophyll measurements (using triplicates). Error bars indicate standard deviations (*n* = 3).

tested for successful co-integration of the mutated NAB1* gene by PCR using two specific PCR amplification experiments covering both, 3′ and 5′ regions to ensure the complete nuclear integration of the mutated NAB1* gene. PCR primer 1 (Fig. 1A) amplified a specific region of the 5′UTR of the *PsaD* promoter including a part of the first intron of the mutated NAB1 (471 bp). PCR primer 2 amplified 808 bp of the second last exon of the mutated NAB1 and includes a part of the 3′ UTR of *PsaD*. As a result we identified 4 transformants (*T7*, *T13*, *T22* and *T69*) in which we successfully demonstrated the integration of the mutagenized NAB1* gene into the genome of *C. reinhardtii* (Fig. 1).

Photometric chlorophyll analysis of cell cultures under mixotrophic growth conditions revealed that all four mutants showed lower total chlorophyll contents and higher Chl *a*/*b* ratios when compared to the control strain (Fig. 1B) both indicative of reduced antenna size. From these strains, *T7* exhibited the most significant phenotype during the complete cultivation period. In cell cultures adjusted to the same cell number *T7* showed the highest increase in Chl *a*/*b* ratio from 2.08 (±0.036 SE) to 2.21 (±0.041 SE) and the strongest reduction in total chlorophyll amount by 20% compared to the parental strain *Stm6Glc4* (Fig. 1B). We consequently selected *T7* for further detailed investigations. This
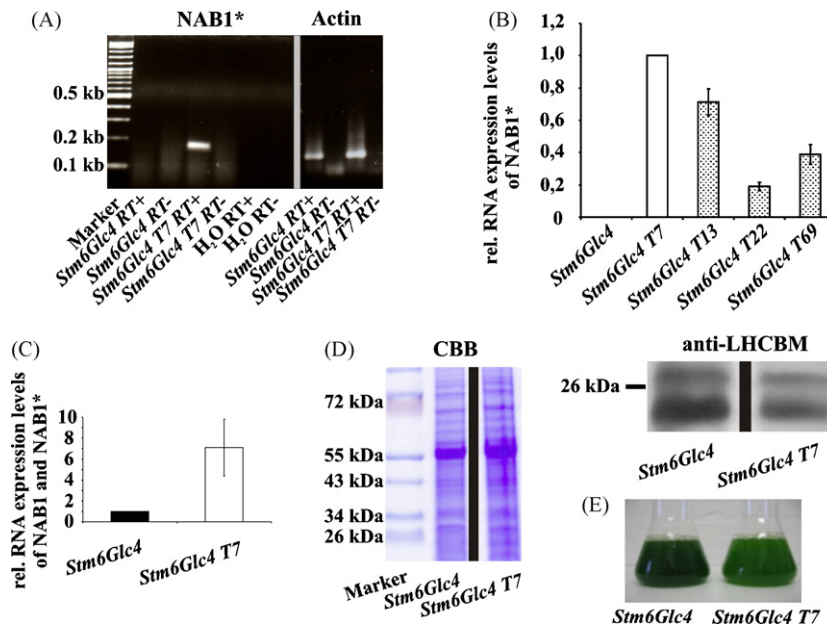
Fig. 2. Evidence for functional NAB1* expression in *T7* and phenotypical analysis. (A) Analysis of NAB1* expression levels by RT-PCR. Signal detection was performed after 29 cycles using primer pair: *qRT-3′NAB*1_fow* (5′cgacaagttgaacaacagcc3′), *qRT-3′NAB*1_rev* (5′cccgtatcaatcagcgaa3′); product size: 150 bp. *β-Actin* was used as a control. (B) Comparative analysis of mutated NAB1* RNA expression levels by Q-RT-PCR in different mutant strains. The expression level of strain *T7* was set to 1. (C) Quantification of the endogenous NAB1 and of the mutated NAB1* transcripts by Q-RT-PCR. The expression level of the parental strain *Stm6Glc4* was set to 1. *β-Actin* transcript levels were used to normalize the NAB1 and NAB1* expression. (D) Immunoblot analysis using antibodies specific for all LHCII isoforms. Total protein extracts derived from *Stm6Glc4* and *T7* were separated by Tris-Tricine-SDS-PAGE (10% (w/v) acrylamide) and transferred to nitrocellulose membranes. Left panel: Coomassie blue stain (loading control), right panel: anti-LHCII immunoblot. (E) Appearance of *T7* (right) and the parental strain *Stm6Glc4* (left) after photoautotrophic growth in HSM medium to the late logarithmic phase. Cell cultures were adjusted to equal cell densities (1.75×10^7 cells mL^{-1}).

phenotype indicated that the transformation of mutated NAB1* into *T7* generated a reduced light-harvesting system consistent with the permanent down-regulation of the LHC gene expression by the constitutive translation repressor NAB1*.

3.2. Evidence for functional NAB1* expression in T7

Functional mRNA transcription of the mutated NAB1* gene was confirmed by RT-PCR (Fig. 2A). PCR amplification of *β-Actin* cDNA was used as a control. Comparative analysis of NAB1* expression rates between the isolated mutant strains by Q-RT-PCR identified mutant *T7* as the strain with the by far highest NAB1* RNA content (Fig. 2B). Quantification of the overall steady state mRNA amount of both, Wild-type NAB1 (which is expressed in the background in all strains) and mutated NAB1* by Q-RT-PCR revealed that the transformant *T7* exhibited a ~6 times higher expression level of total NAB1 than the parental strain *Stm6Glc4* (±2.71 SD), clearly demonstrating the high expression rate of the additionally introduced NAB1* variant in this mutant (Fig. 2C).

SDS-PAGE and LHC II-specific Western analyses were performed with total protein extracts of *Stm6Glc4* and *T7* in order to verify the impact of NAB1* mutation on the LHC II antenna protein level using a polyclonal antibody raised against all LHCII proteins (Andersson et al., 2001; Asakura et al., 2004). The results presented in Fig. 2D show that LHC II proteins in *T7* were markedly reduced compared to those monitored in *Stm6Glc4*. The pale green phenotype in comparison to the parental strain at equal cell density is also consistent with a reduction of the LHCII protein amount (Fig. 2E).

To finally test the overall differences in antenna size we applied chlorophyll fluorescence measurements in the presence of DCMU (to switch off PSII photochemistry). Thus, the rate of fluorescence rise is quantitatively related to the functional antenna size of PSII. The slower rise observed for *T7* in Fig. 3A, visible most prominently at low light (40 μmol m^{-2} s^{-1}), is consistent with an antenna size of ~90% of the parental strain antenna size. This result is in good correlation to our chlorophyll measurements. Taking into account the Chl *b* values as a parameter for LHC antenna size and including the estimation that ~80% of Chl *b* is located in the LHC trimers (Elrad et al., 2002) we could calculate an approximate reduction of antenna size from our chlorophyll measurements by ~15%.

3.3. Characterisation of Stm6Glc4T7 as a mutant with improved photosynthesis under high light

PAM fluorescence measurements were used to investigate the changes in PSII photochemical activity under illumination with increasing light intensities (54 μmol m^{-2} s^{-1}, 350 μmol m^{-2} s^{-1} and 850 μmol m^{-2} s^{-1}). To determine whether the observed reduction of the antenna size contributes to improved photon capture efficiencies, the maximum quantum yield of PSII ($F_v/F_m = (F_m - F_o/F_m)$) and the photosynthetic quantum yield (ΦPSII = $(F'_m - F_t)/F'_m$), where F'_m corresponds to the maximum fluorescence and F_t corresponding to the minimum fluorescence during illumination with actinic light (Maxwell and Johnson, 2000) were recorded (Fig. 3 B). These parameters were measured after transferring cell cultures from dark to the different light intensities. The photosynthetic quantum yield in the light was followed by measuring ΦPSII after a short period of illumination (1 min) for each light intensity, to avoid unwanted photoinhibitory effects and NPQ onset during the illumination. Thus, changes in ΦPSII measured in these experiments should mainly reflect changes in the photochemical conversion capacity, rather than in light dissipation. Consistent with this, although ΦPSII was different in *T7* and *Stm6Glc4*, no significant changes in the F'_m levels were seen between the two strains, while the F_t values were significantly lower in *T7* (not shown).
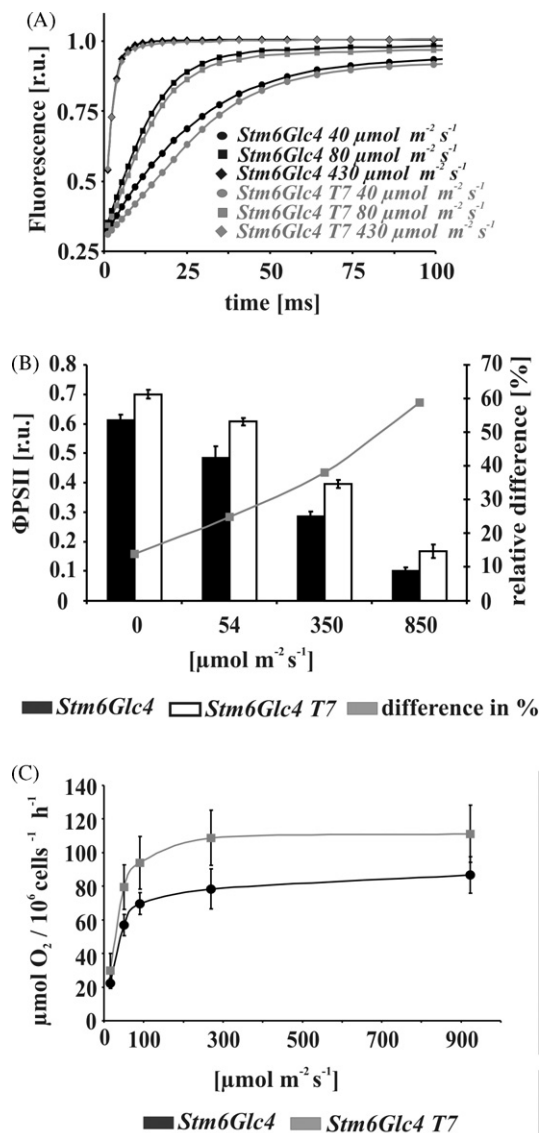
Fig. 3. Evaluation of LHC antenna size and photon conversion efficiency of *T7* by fluorescence parameters. (A) PSII optical section in *T7* and *Stm6Glc4*, as evaluated by the fluorescence rise measured in the presence of DCMU. Cultures were adjusted to equal cell densities (10^7 cells mL^{-1}) and then exposed to actinic light of different intensities. Inhibition of PSII photochemistry at the level of Q$_A$ reduction allowed to estimate the time required for one photon to reach every reaction centre (see text), thus providing a functional estimate of the PSII absorption capacity. (B) F_v/F_m and photosynthetic quantum yield ΦPSII of *T7* and *Stm6Glc4*. Fluorescence parameters F_v/F_m (after dark incubation, 0 μmol m^{-2} s^{-1}) and F_t and F_m during actinic illumination (54 μmol m^{-2} s^{-1}, 350 μmol m^{-2} s^{-1}, 850 μmol m^{-2} s^{-1}) of liquid cultures were recorded. ΦPSII was calculated according to Maxwell and Johnson (2000) (left *y*-axis) (ΦPSII = $(F'_m - F_t)/F'_m$); r.u. = relative units. Error bars = standard error. The curve reflects changes in the relative differences of the fluorescence parameters between *T7* and *Stm6Glc4* (right *y*-axis). (C) Oxygen evolution activity of *T7* and *Stm6Glc4* in relation to the irradiance. Cultures were adjusted to equal cell densities (7.2 × 10^6 cells mL^{-1}) and then exposed to actinic light of different intensities (16–923 μmol m^{-2} s^{-1}) during oxygen evolution measurements using a Clark-type oxygen electrode (*HansaTech*).

Of particular note is that differences in ΦPSII values between parental strain and *T7* (under the same illumination conditions) increased with higher light intensities of photosynthetically active radiation (Fig. 3B) from 14% difference between the two strains in the control measurement over 25% at 54 μmol m^{-2} s^{-1} and 38% at 350 μmol m^{-2} s^{-1} to 59% difference at 850 μmol m^{-2} s^{-1}. These results suggest that the smaller antenna of *T7* leads to a more homogeneous penetration of light into the cultures, thus allowing an increased PCE rate.

Photosynthetic irradiance curves on a per cell basis are presented in Fig. 3C. A higher photosynthetic activity in *T7* compared to the parental strain *Stm6Glc4* was confirmed by light dependent oxygen evolution measurements. In these measurements *T7* showed 25–28% higher maximal photosynthetic activities under saturating light conditions (Fig. 3C). These differences are consistent with the ΦPSII values obtained by PAM measurements (Fig. 3B).

3.4. Stm6Glc4T7 converts light to biomass with high efficiencies

In previous work by others and by us (Polle et al., 2002; Mussgnug et al., 2007) it was demonstrated that a smaller antenna size can prevent photoinhibition under high light conditions, as well as improve light penetration into the bioreactor and thereby increases biomass production efficiencies. We performed phototrophic cultivation experiments in minimal medium (HSM, TAP minus acetate) under high light condition ($700 \, \mu mol \, m^{-2} \, s^{-1}$ and $1000 \, \mu mol \, m^{-2} \, s^{-1}$) to investigate the influence of active LHCII translation repression on high light acclimation. Two independent experiments were performed to compare the growth rates of the antenna mutant *T7* with the growth rates of the parental strains *Stm6* and *Stm6Glc4*. In the first experiment, cells were grown in small scale 200 mL cultivation bottles in HSM medium (Fig. 4A and B). For the second experiment, cells were grown in a 2.4 L closed bioreactor (BioengII) with TAP minus acetate medium to evaluate growth in larger scale (Fig. 4C). As a result, in both experimental approaches cell growth and replication of the mutant *T7* was significant faster compared to the parental strain *Stm6Glc4*. In addition, our results from the large-scale cultivation demonstrated that the strain *T7* is able to grow to higher cell densities (Fig. 4C). Cell culture densities of the antenna mutant in the 200 mL bottles increased within 38 h from $5.97 \times 10^5 \, cells \, mL^{-1}$ to $1.2 \times 10^7 \, cells \, mL^{-1}$ whereas the parental strain reached only $5.72 \times 10^6 \, cells \, mL^{-1}$ after 38 h (Fig. 4A). At variance with the conditions explored in Fig. 3B, it should be noted that this longer exposition to high light conditions probably leads to dissipation of most of the light energy as heat in the parental strain (see e.g. Peers et al., 2007), leading to a loss in productivity. Thus, the improved biomass production efficiency for *T7* can be interpreted in terms of both an increased homogeneity of light distribution within the culture, and a reduced light dissipation from the first layers of cells.

The exponential growth rates of *T7* were also significantly higher compared to parental strain under photoautotrophic conditions (with $0.028 \, \Delta \, cells \, mL^{-1} \, h^{-1}$ *versus* $0.018 \, \Delta \, cells \, mL^{-1} \, h^{-1}$). From our data we calculated an average 53% improved mid log growth phase for *T7* in comparison to *Stm6Glc4* (Fig. 4B). In good correlation with this results, total chlorophyll content was decreased by ~20% in the mutant (~$27.75 \, mg \, L^{-1}$) compared to *Stm6Glc4* (~$35.75 \, mg \, L^{-1}$) during the whole cultivation experiment (Fig. 4A). Furthermore cultivation experiments in a 2.4 L bioreactor under elevated light condition ($1000 \, \mu mol \, m^{-2} \, s^{-1}$) revealed a strong lag in cell growth in the control strain (Fig. 4C). This is consistent with photodamage occurring in this strain at the initial step of growth. Maximum densities of *T7* cultures grown under photoautotrophic conditions were obtained after 119 h ($2.136 \, g \, L^{-1}$), a time point where the control strain had only been able to grow to 37% of its maximal dry weight (dw) ($0.794 \, g \, L^{-1}$) (Fig. 4C).

In addition, the maximal control strain dw of $1.57 \, g \, L^{-1}$ after ~150 h of cultivation was far below the *T7* dw of $2.038 \, g \, L^{-1}$ after 145 h. This suggests that either light stress occurred in *Stm6Glc4* during exponential growth, or that enhanced light dissipation decreased their overall photochemical light conversion.

In summary we conclude that the de-regulation of LHC translation via a permanently active NAB1 repressor caused a decreased LHC antenna size and an improved light transmission into the cell culture, leading to higher light conversion efficiencies. Faster
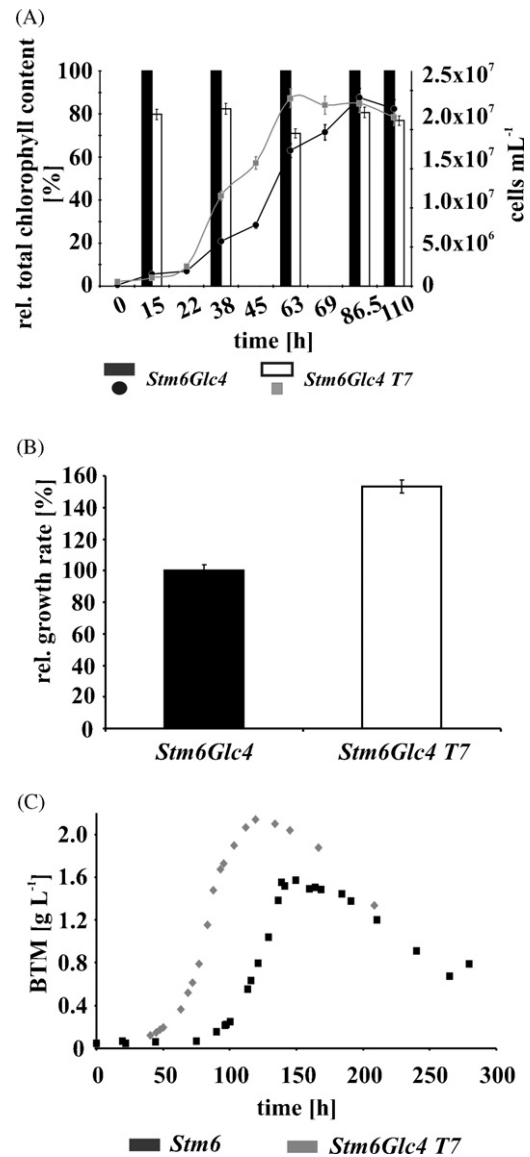
Fig. 4. Evidence for improved light to biomass conversion of *T7* and *Stm6Glc4* under high light conditions. (A) Phototrophic growth of *T7* and *Stm6Glc4* observed under continuous high light conditions ($700 \, \mu mol \, m^{-2} \, s^{-1}$) in high salt medium in an experimental setup with 200 mL cultures over 110 h. Right *y*-axis: cell densities per mL. Left *y*-axis: chlorophyll values. The total chlorophyll content (in %) was measured in relative amounts to parental strain (=100%). (B) Growth rates within in the exponential phase observed under phototrophic high light conditions (high salt medium, $700 \, \mu mol \, m^{-2} \, s^{-1}$). The growth rate was determined by the increase of the cell densities per hour and depicted in percentage. Error bars indicate the standard error in percent of three independent growth experiments. (C) Phototrophic growth of *T7* and *Stm6* observed under continuous high light conditions ($1000 \, \mu mol \, m^{-2} \, s^{-1}$) in minimal medium (TAP minus acetate) using a 2.4 L stirred tank reactor (BioengII) over time period of 300 h. The presented data set reflect the result of a single growth experiment which has been subsequently confirmed by two biological replicates.

growth rates and higher cell densities were obtained in minimal medium and indicate that *T7* has got advantageous growth parameter for large-scale microalgae cultivation under high light conditions (between 700 and $1000 \, \mu mol \, m^{-2} \, s^{-1}$).

4. Discussion

One of the major problems in the efficient use of microalgae to convert sun light energy into biomass and eventually into bioenergy is connected to the losses which occur during high light illumination of dense cell cultures in closed bioreactors. Under these

outdoor like conditions which cell cultures have to acclimate to, most of the light energy is dissipated by the LHC antenna system of the cell closer to the illuminated surface therefore preventing the efficient penetration of the light deeper into the culture (Polle et al., 2002).

Here we have demonstrated proof-of-concept that biotechnology applications which include the manipulation of the size and composition of light-harvesting antenna complexes at photosystem II can increase the efficiency of sunlight to biomass conversion. The relevance of an efficient LHC antenna size is of particular importance for future outdoor cultivation of microalgae in closed bioreactor systems where high density cell cultures are forced to acclimate to conditions of uneven light distribution within the reactor, ranging from light intensities higher than $1000\,\mu mol\,m^{-2}\,s^{-1}$ at the surface of the reactor down to only dim light conditions inside the reactor.

This uneven light distribution problem can be overcome by using cell cultures with smaller antenna sizes and less chlorophyll content which can be then packed to high cell density cultures, still allowing good light penetration into the inner sections of the reactor. Our results demonstrated that the C. reinhardtii strain T7 shows advantageous properties in regard to reaching these targets. Under 700–$1000\,\mu mol\,m^{-2}\,s^{-1}$ high light conditions, strain T7 exhibited 10–20% reduced levels of LHCII proteins but was shown to grow with a much higher efficiency using strictly phototrophic cultivation conditions (no external fixed carbon source provided) when compared with the control strain (Fig. 4).

In previous experiments we already demonstrated the impact of the overall light-harvesting antenna size on the photosynthetic efficiency in the C. reinhardtii strain Stm3LR3 (Mussgnug et al., 2007). In this strain, the complete LHC antenna size was dramatically downregulated by a targeted RNAi approach. In Stm3LR3 both, the PSII and the PSI antenna genes were strongly affected (isoform dependent, the mRNA levels were reduced to 0.1–26%) which resulted in a chlorophyll content of around 32% compared to the control strain. This mutant showed an increase in photosynthetic conversion efficiency when cultivated under high light (Mussgnug et al., 2007). However, it is well documented that RNAi induced phenotypes can become unstable after some time (Yamasaki et al., 2008). In this work we intended to reduce the LHC antenna size by repressing the LHC protein translation by permanently active NAB1 (Mussgnug et al., 2005). The advantage of this approach is the repression of antenna protein synthesis by a genetically engineered translation repressor protein, which circumvents the application of RNAi techniques. In future applications this manipulation technique should therefore be more stable in the long term. T7 could serve as a suitable flexible strain capable to acclimate its antenna size to the desired light conditions by use of an inducible promoter system controlling the induction of NAB1* gene transcription. Post-transcriptional regulation of LHCBM genes during high light acclimation in the unicellular green alga C. reinhardtii was demonstrated to induce a strong reduction of LHCII protein levels (Durnford et al., 2003). NAB1 was identified as the cytosolic translation repressor that sequestrates LHCBM mRNAs in sub-polysomal messenger ribonucleoprotein complexes, thus separating such transcripts from the factors required for translation initiation. Interestingly, besides general LHCBM message recognition, this protein shows a strong selectivity towards distinct isoform mRNAs of the highly homologous LHCBM gene family. The repressor activity of NAB1 is modulated by a reversible thiol switch within its C-terminal domain and recent data suggest that light triggers reversible thiol modification of the protein (Wobbe et al., 2008a, Wobbe et al., unpublished).

The C-terminal RRM domain of NAB1 harbours two cysteine residues at amino acid positions 181 and 226. In a recent work we confirmed the relevance of reversible NAB1 cysteine oxidation

for the redox-regulation of its activity in vivo by replacing both cysteines with serines using site-directed mutagenesis approaches (Wobbe et al., unpublished). Examined cysteine double mutants exhibited a reduced antenna at PSII caused by a perturbed NAB1 deactivation mechanism.

We now used these new results on LHC regulation via NAB1 to successfully transfer this approach to our recently engineered high H_2 production strain Stm6Glc4 (Doebbe et al., 2007). The screening procedure (Fig. 1) and the characterisation of the most promising candidate T7 (Fig. 2) clearly confirmed that a permanently active variant of NAB1 causes a ~10–20% smaller LHC antenna phenotype (Fig. 2). Photosynthetic efficiency and phototrophic growth experiments under high light conditions clearly provided further evidence that a controlled reduction of the PSII antenna size by less than 20% is sufficient for a remarkable increase in photosynthetic efficiency of PSII and an increasing insensitivity against high light photoinhibition reflected by a slower decrease in ΦPSII rates (Fig. 3B). As a result, less captured sunlight energy is wasted as heat or fluorescence. The overall consequence is a faster biomass production with cell cultures reaching already their maximal cell density ~24 h earlier compared to the control strain (Fig. 4).

In conclusion, the possibility of acclimating the antenna size to higher light conditions and to improve homogeneous absorption into closed reactor systems via the regulation of LHC translation provides us with a new flexible tool of a tuneable light antenna system on the molecular level. Control of the antenna can be introduced using suitable promoter systems for NAB1* expression to enable algae cultivation in closed bioreactor systems under varying light conditions.

Furthermore, the phenotype of strain T7 perfectly underlines earlier results obtained with the RNAi strain Stm3LR3 (Mussgnug et al., 2007) and will have important implications for biotechnological applications in which photosynthetic micro-organisms are increasingly used for large-scale algal culturing as an alternative plant biomass source (Pulz and Gross, 2004; Hankamer et al., 2007).

References

Anderson, J.M., Andersson, B., 1988. The dynamic photosynthetic membrane and regulation of solar energy conversion. Trends Biochem. Sci. 13, 351–355.

Andersson, J., Rupprecht, J., Walters, R.G., Horton, P., Jansson, S., 2001. Antisense inhibition of the photosynthetic antenna proteins CP29 and CP26: implications for the mechanism of protective energy dissipation. Plant Cell 13, 1193–1204.

Asakura, Y., Hirohashi, T., Kikuchi, S., Belcher, S., Osborne, E., Yano, S., Terashima, I., Barkan, A., Nakai, M., 2004. Maize mutants lacking chloroplast FtsY exhibit pleiotropic defects in the biogenesis of thylakoid membranes. Plant Cell 16, 201–214.

Chomczynski, P., Sacchi, N., 1987. Single-step method of RNA isolation by acid guanidine thiocyanate-phenol-chloroform extraction. Anal. Biochem. 162, 156–159.

Doebbe, A., Rupprecht, J., Beckmann, J., Mussgnug, J.H., Hallmann, A., Hankamer, B., Kruse, O., 2007. Functional integration of the HUP1 hexose symporter gene into the genome of C. reinhardtii: impacts on biological H(2) production. J. Biotechnol. 131, 27–33.

Durnford, D.G., Falkowski, P.G., 1997. Chloroplast redox regulation of nuclear gene transcription during photoacclimation. Photosynth. Res. 53, 229–241.

Durnford, D.G., Price, J.A., McKim, S.M., Sarchfield, M.L., 2003. Light-harvesting complex gene expression is controlled by both transcriptional and post-transcriptional mechanisms during photoacclimation in Chlamydomonas reinhardtii. Physiol. Plantarum 118, 193–205.

Elrad, D., Grossman, A.R., 2004. A genome's-eye view of the light-harvesting polypeptides of Chlamydomonas reinhardtii. Curr. Genet. 45, 61–75.

Elrad, D., Niyogi, K.K., Grossman, A.R., 2002. A major light-harvesting polypeptide of photosystem II functions in thermal dissipation. Plant Cell 14, 1801–1816.

Escoubas, J.M., Lomas, M., Laroche, J., Falkowski, P.G., 1995. Light-intensity regulation of cab gene-transcription is signaled by the redox state of the plastoquinone pool. Proc. Natl. Acad. Sci. U.S.A. 92, 10237–10241.

Fischer, N., Rochaix, J.D., 2001. The flanking regions of PsaD drive efficient gene expression in the nucleus of the green alga *Chlamydomonas reinhardtii*. Mol. Genet. Genom. 265, 888–894.

Flachmann, R., Kühlbrandt, W., 1995. Accumulation of plant antenna complexes is regulated by post-transcriptional mechanisms in tobacco. Plant Cell 7, 149–160.

Hankamer, B., Lehr, F., Rupprecht, J., Mussgnug, J.H., Posten, C., Kruse, O., Hankamer, B., 2007. Photosynthetic biomass and H(2) production by green algae: from bio-engineering to bioreactor scale-up. Physiol. Plantarum 131, 10–21.

Harris, E.H., 1989. In: Govanovich, H.B. (Ed.), The Chlamydomonas Sourcebook—A Comprehensive Guide to Biology and Laboratory Use. Academic Press, Inc., San Diego, California.

Joliot, P., Joliot, A., 2005. Quantification of cyclic and linear flows in plants. Proc. Natl. Acad. Sci. U.S.A. 102, 4913–4918.

Kindle, K.L., 1990. High frequency nuclear transformation of *Chlamydomonas reinhardtii*. Proc. Natl. Acad. Sci. U.S.A. 87, 1228–1232.

Kruse, O., Rupprecht, J., Bader, K.P., Thomas-Hall, S., Schenk, P.M., Finazzi, G., Hankamer, B., 2005. Improved photobiological H(2) production in engineered green algal cells. J. Biol. Chem. 280, 34170–34177.

Lindahl, M., Yang, D.H., Andersson, B., 1995. Regulatory proteolysis of the major light-harvesting chlorophyll *a/b* protein of photosystem II by a light-induced membrane-associated enzymatic system. Eur. J. Biochem. 231, 503–509.

Maxwell, K., Johnson, G.N., 2000. Chlorophyll fluorescence—a practical guide. J. Exp. Bot. 51, 659–668.

Maxwell, D.P., Laudenbach, D.E., Huner, N.P.A., 1995. Redox regulation of light-harvesting complex II and *cab* mRNA abundance in *Dunaliella salina*. Plant Physiol. 109, 787–795.

Melis, A., 1999. Photosystem-II damage and repair cycle in chloroplasts: what modulates the rate of photodamage in vivo? Trends Plant Sci. 4, 130–135.

Müller, P., Li, X.P., Niyogi, K.K., 2001. Non-photochemical quenching. A response to excess light energy. Plant Physiol. 125, 1558–1566.

Millar, A.J., Straume, M., Chory, J., Chua, N.H., Kay, S.A., 1995. The regulation of circadian period by phototransduction pathways. Arabidopsis. Sci. 267, 1163–1166.

Mussgnug, J.H., Wobbe, L., Elles, I., Claus, C., Hamilton, M., Fink, A., Kahmann, U., Kapazoglou, A., Mullineaux, C.W., Hippler, M., Nickelsen, J., Nixon, P.J., Kruse, O., 2005. NAB1 is an RNA binding protein involved in the light regulated differential expression of the light-harvesting antenna of *Chlamydomonas reinhardtii*. Plant Cell 17, 3409–3421.

Mussgnug, J.H., Thomas-Hall, S., Rupprecht, J., Foo, A., Klassen, V., McDowall, A., Schenk, P.M., Kruse, O., Hankamer, B., 2007. Engineering photosynthetic light capture: impacts on improved solar energy to biomass conversion. Plant Biotechnol. J. 5, 802–814.

Neidhardt, J., Benemann, J.R., Zhang, L.P., Melis, A., 1998. Photosystem-II repair and chloroplast recovery from irradiance stress: relationship between chronic photoinhibition, light-harvesting chlorophyll antenna size and photosynthetic productivity in *Dunaliella salina* (green algae). Photosynth. Res. 56, 175–184.

Nelson, J.A.E., Savereide, P.B., Lefebvre, P.A., 1994. The *Cry1* Gene in *Chlamydomonas reinhardtii*—structure and use as a dominant selectable marker for nuclear transformation. Mol. Cell. Biol. 14, 4011–4019.

Nguyen, A.V., Thomas-Hall, S.R., Malnoë, A., Timmins, M., Mussgnug, J.H., Rupprecht, J., Kruse, O., Hankamer, B., Schenk, P.M., 2008. The transcriptome of photo-biological hydrogen production induced by sulphur deprivation in the green alga *Chlamydomonas reinhardtii*. Eukaryot. Cell. 7, 1965–1979.

Peers, G., Troung, T., Elrad, D., Grossman, A., Niyogi, K., 2007. A non photochemical quenching mutant of *Chlamydomonas* reveals a role for Li818/LHCSR proteins. Photosynth. Res. 91, 250.

Polle, J.E.W., Kanakagiri, S., Jin, E., Masuda, T., Melis, A., 2002. Truncated chlorophyll antenna size of the photosystems—a practical method to improve microalgal productivity and hydrogen production in mass culture. Int. J. Hydrogen Energy 27, 1257–1264.

Polle, J.E.W., Kanakagiri, S.D., Melis, A., 2003. tla1, a DNA insertional transformant of the green alga *Chlamydomonas reinhardtii* with a truncated light-harvesting chlorophyll antenna size. Planta 217, 49–59.

Prince, R.C., Kheshgi, H.S., 2005. The photobiological production of hydrogen: potential efficiency and effectiveness as a renewable fuel. Crit. Rev. Microbiol. 31, 19–31.

Pulz, O., Gross, W., 2004. Valuable products from biotechnology of microalgae. Appl. Microbiol. Biotechnol. 65, 635–648.

Sambrook, J., Russel, D.W., 2001. Molecular Cloning: A Laboratory Manual, third ed. Cold Spring Harbor Laboratory Press, Cold Spring Harbor, NY.

Schägger, H., Jagow, G., 1987. Tricin-sodium-dodecylsulfate polyacrylamide gel electrophoresis for the separation of proteins in the range from 1–100 kDa. Anal. Biochem. 166, 368–379.

Stauber, E.J., Fink, A., Markert, C., Kruse, O., Johanningmeier, U., Hippler, M., 2003. Proteomics of *Chlamydomonas reinhardtii* light-harvesting proteins. Eukaryot. Cell 2, 978–994.

Sueoka, N., Chiang, K.S., Kates, J.R., 1967. Deoxyribonucleic acid replication in meiosis of *Chlamydomonas reinhardtii* I. Isotopic transfer experiments with a strain producing eight zoospores. J. Mol. Biol. 25, 44–67.

Towbin, H., Staehelin, T., Gordon, J., 1979. Electrophoretic transfer of proteins from polyacrylamide gels to nitrocellulose sheets—procedure and some applications. Proc. Natl. Acad. Sci. U.S.A. 76, 4350–4354.

Turkina, M.V., Kargul, J., Blanco-Rivero, A., Villarejo, A., Barber, J., Vener, A.V., 2006. Environmentally modulated phosphoproteome of photosynthetic membranes in the green alga *Chlamydomonas reinhardtii*. Mol. Cell Proteom. 5, 1412–1425.

Wobbe, L., Schwarz, C., Nickelsen, J., Kruse, O., 2008a. Translational control of photosynthetic gene expression in phototrophic eukaryotes. Physiol. Plant 133, 507–515.

Yamasaki, T., Miyasaka, H., Ohama, T., 2008. Unstable RNAi effects through epigenetic silencing of an inverted repeat transgene in *Chlamydomonas reinhardtii*. Genetics 180, 1927–1944.

Yang, D.H., Andersson, B., Aro, E.M., Ohad, I., 2001. The redox state of the plastoquinone pool controls the level of the light-harvesting chlorophyll a/b binding protein complex II (LHC II) during photoacclimation—cytochrome b(6)f deficient *Lemna perpusilla* plants are locked in a state of high-light acclimation. Photosynth. Res. 68, 163–174.